Published OnlineFirst June 1, 2011; DOI: 10.1158/1535-7163.MCT-10-1087

Molecular Cancer Therapeutics

Phenotypic Reversion of Invasive Neurofibromin-Deficient Schwannoma by FTS: Ras Inhibition Reduces BMP4/Erk/Smad Signaling

Batya Barkan, Yoel Kloog and Marcelo Ehrlich

Mol Cancer Ther 2011;10:1317-1326. Published OnlineFirst June 1, 2011.

Published OnlineFirst June 1, 2011; DOI: 10.1158/1535-7163.MCT-10-1087

Therapeutic Discovery

Molecular Cancer Therapeutics

Phenotypic Reversion of Invasive Neurofibromin-Deficient Schwannoma by FTS: Ras Inhibition Reduces BMP4/Erk/Smad Signaling

Batya Barkan[1], Yoel Kloog[1], and Marcelo Ehrlich[2]

Abstract

Neurofibromin-deficient ($Nf1^{-/-}$) malignant peripheral nerve sheath tumors (MPNST) are highly invasive, refractory to chemotherapy, and characterized by overactivated Ras. Ras activates mitogenic pathways and regulates morphogenic programs—such as those induced by bone morphogenetic proteins (BMP) and TGF-β. The role of such a cross-talk in determining the phenotype and transformation potential of MPNSTs is unknown. Here, we used MPNST cell lines and selective Ras inhibition with *S-trans,trans*-farnesylthiosalicylic-acid (FTS; salirasib) in conjunction with specific inhibitors of TGF-β and BMP signaling. FTS perturbed signaling of BMP4 and TGF-β1 to Smad-dependent and Erk-dependent pathways. Furthermore, FTS inhibited motility and spreading, reduced the gelatinase secretion, eliminated the expression and activation of regulators of cell–matrix interaction, and altered gene expression. These phenomena are indicative of a phenotypic reversion of NF1-defficient cells by FTS. Inhibition of BMP4 and TGF-β by noggin and SB-431542, respectively, mimicked the FTS-mediated effects on adhesion, spreading, and cell morphology. This strongly suggests that a cross-talk among TGF-β superfamily ligands and Ras plays a significant role in the transformation of $NF1^{-/-}$ MPNSTs. Our results support the therapeutic potential of FTS, in conjuncture with BMP and TGF-β pathway inhibitors, toward the inhibition of mitogenic and morphogenic signaling pathways and the alleviation of NF1 symptoms. *Mol Cancer Ther; 10(8); 1317–26. ©2011 AACR.*

Introduction

Phenotypic alterations and dedifferentiation of cancer cells are critical in malignancy and increase the invasive/metastatic attributes of tumors (1). Chronically active Ras drives tumor progression through deregulation of proliferation and phenotypic transformation (2). Altered phenotypic regulation of cancers cells, such as the epithelial-to-mesenchymal transition (EMT) of epithelial tumors, results from the integration of developmental or morphogenic signaling pathways with those induced by deregulated Ras (3).

TGF-β and bone morphogenetic proteins (BMP), essential in embryogenesis, induce EMT in development and disease and stimulate metastasis (4, 5). BMPs regulate neural crest migration (6), alter cell morphology, and increase cell motility and invasiveness in colon, prostate, ovarian, and pancreatic cancers (7, 8). TGF-β, despite its initial role as a tumor suppressor, establishes an undifferentiated phenotype and associates with progressed stages of tumorigenesis (9).

BMPs and TGF-βs bind and activate heteromeric complexes of receptor serine/threonine kinases, and lead to the phosphorylation/activation of pathway-specific Smad proteins (Smads2/3 for TGF-β and Smads1/5/8 for BMPs). Activated Smads oligomerize with Smad4, translocate to the nucleus, and mediate transcriptional activation and/or repression (10, 11). TGF-β and BMP receptors activate additional kinase cascades, such as those regulated by Ras (10). Ras activation may promote, inhibit, or modify TGF-β and BMP signaling, depending on cellular context and signal intensity (3, 11).

Overactivation of Ras stems from gene mutations, overactivation of receptors that activate Ras, and/or reduced activity of Ras-GTPase activating proteins (Ras-GAP; ref. 12). A prototypical example of the latter occurs in neurofibromatosis type 1 (NF1), an autosomal inherited disease with a 1:3,000 prevalence (13). The hallmark of NF1 is the neurofibroma, a peripheral nerve

Authors' Affiliations: Departments of [1]Neurobiology and [2]Cell Research and Immunology, The George S. Wise Faculty of Life Sciences, Tel Aviv University, Tel Aviv, Israel

Note: Supplementary material for this article is available at Molecular Cancer Therapeutics Online (http://mct.aacrjournals.org/).

Y. Kloog is the incumbent of the Jack H. Skirball Chair in Applied Neurobiology.

This work partially fulfills the requirements for a PhD thesis (Tel Aviv University) by B. Barkan.

Corresponding Author: Yoel Kloog, Department of Neurobiology, Tel Aviv University, Tel Aviv, 69978 Israel. Phone: 9723-640-9699; Fax: 9723-640-7643; E-mail: kloog@post.tau.ac.il

doi: 10.1158/1535-7163.MCT-10-1087

Published OnlineFirst June 1, 2011; DOI: 10.1158/1535-7163.MCT-10-1087

benign tumor comprised of transformed Schwann cells (14). Neurofibromas undergo transformation into aggressive and chemotherapy-resistant malignant peripheral nerve sheath tumors (MPNST), which are prone to live-threatening metastasis (15). Loss of neurofibromin Ras-GAP activity is associated with increased Ras-GTP and overactivation of Ras effectors (16), leading to NF1 (17, 18). The role of Ras in NF1-based malignancy suggests that Ras inhibitors, such as *S-trans,trans*-farnesylthiosalicylic acid (FTS; salirasib) that interferes with Ras-membrane anchorage (19), are an efficient therapeutic approach. Importantly, FTS interferes with the transformed phenotype of NF1-associated MPNST cell lines *in vitro* and *in vivo* (20).

The tumorigenicity of NF1 cells is influenced by modifications to Ras/Raf/Erk signaling (21), the absence of axon–Schwann cell interactions (21), and by the infiltration of TGF-β–secreting $NF1^{+/-}$ mast cells to their microenvironment (22). However, the cross-talk between Ras and TGF-β superfamily signaling in NF1-deficient shwannomas is unexplored. We report here that FTS reduced the spreading and motility of NF1-deficient MPNSTs, altered their transcriptome and the expression of Schwann-cell markers, reduced BMP4 expression, and inhibited the basal and ligand-mediated activation of Smad1/5/8 and Smad3; all in accord with an FTS-induced phenotypic reversion of invasive NF1-deficient schwannomas via alterations to Ras and TGF-β superfamily signaling.

Materials and Methods

Cell culture

ST88-14, T265P21, and STS26T cells were from Dr. Nancy Ratner [Cincinnati Children's Hospital and Medical Center, University of Cincinnati; received in 2002; immediately frozen, used at a low passage number (less than 4 months in culture)]. They were routinely checked for *Mycoplasma*, maintained, and genetically analyzed [exon-specific PCR amplification, denaturing high-performance liquid chromatography, and sequencing (20)]. Plating was at 0.75×10^6 cells (10-cm dish), 15×10^4 cells (6-well plate), and 7,500 cells (18-mm glass coverslip).

Rac-GTP assay

Rac-GTP was pulled down with glutathione–sepharose transferase conjugated Rac-binding domain of PAK1 (GST–PBD; Rac-binding domain of PAK1-conjugated beads; ref. 23). Cell lysates [500 μg protein in 25 mmol/L HEPES (pH 7.5) 150 mmol/L NaCl, 1% NP40, 10% glycerol, 10 mmol/L $MgCl_2$, 1 mmol/L EDTA, and protease inhibitors] were incubated with glutathione–sepharose beads/GST–PBD (1 hour, 4°C, and 500 μg), separated by SDS-PAGE, and analyzed by immunoblotting (24).

Cell elongation analysis

The ratio between length (largest distance between points) and width (largest perpendicular line to the length) of individual, randomly selected rhodamine/phalloidin–labeled cells (imaged with Nikon ECLIPSE TE2000-S, CoolSNAP^{HQ}, ×60 magnification; Image-Pro Plus) was determined with ImageJ software (NIH).

Spreading assay

Cells, treated with FTS or inhibitors (see legends), were harvested by trypsinization, washed, left to recover (30 minutes, 37°C), replated on fibronectin-coated 35–mm plates (20 μg/mL fibronectin, 1×10^5 cells per plate), fixed, stained (phalloidin/Hoechst), and imaged (randomly selected fields, Zeiss 200M microscope, ×10 lens, HQ2-Photometrics camera, SlideBook software). Cells were identified by intensity based segmentation (phalloidin fluorescence), defined as objects, and measured (area, SlideBook software).

Wound-healing assay

Confluent cells (24 hours postplating) were treated with FTS [18 hours, 10 μmol/L, 0.5% fetal calf serum (FCS)], mytomycin C (18 hours, 10 μg/mL, 0.5% FCS), or vehicle [0.1% dimethyl sulfoxide (DMSO)]. Cell monolayers were scratched (3 scratches per plate), washed, and imaged by phase contrast microscopy (×10 objective; after 0, 8, and 24 hours). Each condition was measured at 9 different areas. Experiments were in duplicates, yielding 18 sets of distance measurements. Gap widths were measured with ImageJ.

Zymography

Cells [0.75×10^6 cells; Dulbecco's Modified Eagle's Medium (DMEM)/5% FCS] were treated with FTS (48 hours, 75 μmol/L) or 0.1% DMSO. Media from equal numbers of cells were separated on nonreducing 8% SDS-PAGE/0.1% gelatin. Gels were washed with 2.5% Triton X-100, 50 mmol/L, and Tris-HCl; incubated with 50 mmol/L Tris-HCl, 0.02% azide, and 10 mmol/L $CaCl_2$ (48 hours, 37°C); and stained with Coomassie Blue R250.

Gene expression profiling

Cells treated with FTS (75 μmol/L and DMEM/5% FCS) or DMSO (0.1% DMEM/5% FCS) were lysed (TRIzol) and analyzed with Affymetrix Human Genome U133A according to the manufacture instructions. Hybridization (10 μg cRNA; overnight) was carried out with spike controls. The Mas5 algorithm was used for gene analysis. When comparing FTS-treated and control cells, $P \leq 0.05$ was considered significant.

Results

The Ras inhibitor FTS reverses the migratory/invasive phenotype of ST88-14 cells

The effects of FTS (10 μmol/L, overnight) on ST88-14 cells' motility was assayed by following the closure of a pipette tip-inflicted wound on a confluent monolayer of serum-starved cells. The absence of serum minimizes cell replication and avoids concentration, compromising binding of FTS to serum elements (25). Of note, prolonged

Published OnlineFirst June 1, 2011; DOI: 10.1158/1535-7163.MCT-10-1087

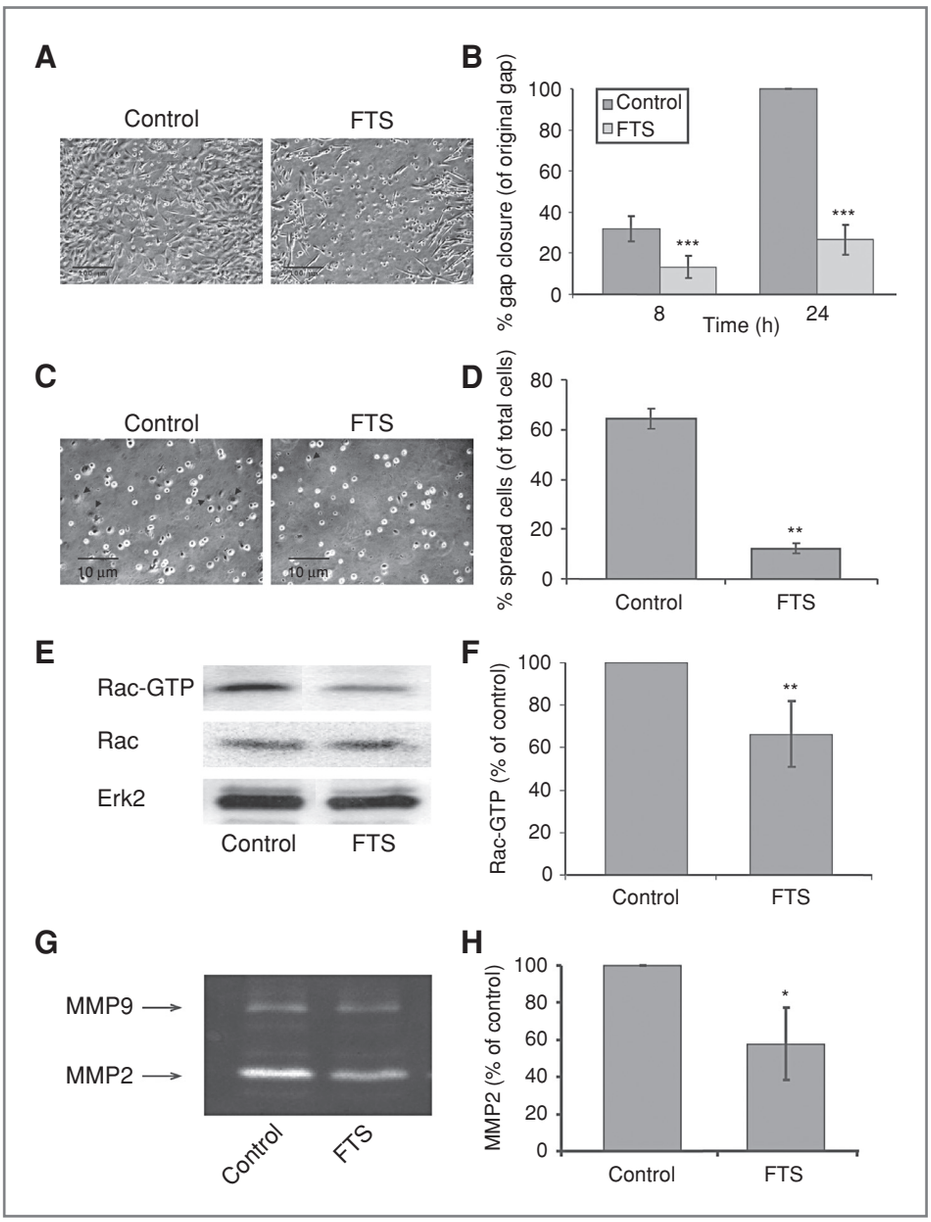

Figure 1. FTS reverses the migratory phenotype of ST88. A, confluent ST88-14 cells, treated with FTS (18 hours, 10 μmol/L, 0.5% FCS) or vehicle, were wounded with a fine pipette tip and imaged after 0, 8, and 24 hours. Micrographs depict typical fields at 24 hours. Bar, 100 μm. B, quantification of gap closure of a typical experiment; vehicle-treated cells (dark gray), FTS-treated cells (light gray; ***, $P < 0.001$; $n = 6$). C, ST88-14 cells, treated with FTS (48 hours, 75 μmol/L, 5% FCS) or vehicle, were trypsinized, reseeded on fibronectin-coated dishes (2 hours, 5% FCS), and imaged by phase contrast microscopy. Micrographs are representative fields (×10 magnification; arrows indicate spread cells; bar, 100 μm). D, graph depicts the percentage of spread cells per condition (**, $P < 0.01$; $n = 3$). E, typical immunoblots α-Rac-GTP (top), α-tRac (bottom), and α-tErk2 (used here and thereafter as loading control) of ST88-14 cells were, treated with FTS (48 hours, 75 μmol/L, 5% FCS) or vehicle and subjected to Rac-GTP pull down. F, quantification of Rac-GTP levels (% of control; **, $P < 0.01$; $n = 4$). G, representative zymography gel of cells treated with FTS (48 hours, 75 μmol/L, 5% FCS) or vehicle. H, quantification of the gelatinase activity of MMP2 in the different media (relative to control; *, $P < 0.05$; $n = 3$).

incubations with 20 μmol/L FTS or more in the absence of serum induces apoptosis (26). Gap width at 0, 8, and 24 hours postwounding was calculated from phase contrast images (Fig. 1A, representative fields at 24 hours; Fig. 1B, quantification). Both at 8 and 24 hours, FTS significantly reduced wound closure ($P < 0.001$). To rule out FTS-mediated effects on cell proliferation as the sole cause of this inhibition, analogous experiments were carried out with mitomycin C (10 μg/mL). Mitomycin C had no effect on wound closure, but had a small additive effect over FTS alone (Supplementary Fig. S1A and B). Taken together, these results suggest that FTS reduces wound closure through mechanisms distinct from cell proliferation. Similarly, the spreading of ST88-14 cells was reduced by FTS (Fig. 1C and D; 5-fold reduction in the percentage of spread cells; $P < 0.01$; $n = 3$).

FTS inhibits active Ras-GTP and its downstream effectors in NF1-deficient MPNSTs (20). Ras regulates Rac and cell–matrix interactions through Tiam1 (27). Overactivated Rac directly contributes to the hyperproliferation of NF1-deficient mast cells *in vitro* and *in vivo* (28). Here, FTS (48 hours) reduced Rac-GTP levels (to ~66% of control; $P < 0.01$; Fig. 1E and F). Thus, the motile invasive phenotype of ST88-14 is sensitive to FTS inhibition of Ras and its downstream effector Rac.

Next, we determined the sensitivity of the gelatinase activity of ST88-14 cells, a measure of the invasive phenotype mediated by matrix metalloproteinases (MMP), to

Published OnlineFirst June 1, 2011; DOI: 10.1158/1535-7163.MCT-10-1087

FTS. Conditioned media of ST88-14 cells, untreated or treated with FTS (48 hours), were examined by zymography. FTS significantly reduced MMP2 activity (to ~58% of control, $P < 0.05$, $n = 3$; Fig. 1G and H) and had smaller effect on MMP9 secretion. Our results suggest that Ras regulates ST88-14 cell motility, spreading, and gelatinase secretion, all of which are inhibited by FTS.

FTS inhibits regulators of spreading and invasiveness

Activated Ras may also regulate MPNST invasiveness and spreading through alterations to the focal adhesion kinase (FAK) and additional components of the focal adhesion complex (29). Indeed, *Nf1*$^{-/-}$ fibroblasts have more phosphorylated FAK (p-FAK) and stress fiber structures than normal cells (30). Moreover, inactivation of FAK in Schwann cells decreases proliferation (31). FTS (48 hours; Fig. 2A and B) induced a mild but significant reduction in FAK phosphorylation on Tyr397 (to ~70% of control, $P < 0.05$, $n = 6$) and reduced the typical distribution of p-FAK to discrete structures at the ventral membrane of the cell (Fig. 2C).

An additional regulator of cell migration, spreading, invasiveness and metastasis, and a specific and necessary effector of FAK is HEF1 (HEF1/NEDD9/Cas-L; refs. 32, 33). In accord with the above-described phenomena, FTS (48 hours) strongly reduced the expression of HEF1 (Fig. 2D and E). In untreated cells, the predominant HEF1 species was p115, indicating a correlation between HEF1 phosphorylation and the high degree of spreading, migration, and FAK phosphorylation observed in ST88-14 cells (Fig. 2). FTS strongly reduced the expression of both the p105 and the hyperphosphorylated p115 forms of HEF1 (to 26% and 25% of control, respectively, $P < 0.001$, $n = 3$; Fig. 2D and E) and of HEF1 mRNA [to 26% of control by quantitative real-time PCR (qRT-PCR), $P < 0.001$, $n = 4$; Fig. 2F]. We suggest that activated Ras positively regulates the expression of HEF1, contributing to the invasive phenotype of NF1-deficient cells.

FTS modifies the transcriptome of ST88-14 cells

Next, we assessed for FTS-induced alterations to the transcriptome of ST88-14 cells. FTS altered the expression of 3,166 genes by more than 2-fold (1,427 upregulated, 1,739 downregulated; data are available in the ArrayExpress database (34), accession no. E-MEXP-2766). Prominent upregulated genes were related to Schwann-cell differentiation such as myelin oligodendrocyte glycoprotein (97-fold increase), collagen VI-α1 (104-fold increase), and osteopontin (15-fold increase). Moreover, the inhibitory Smad6 was upregulated by 29-fold. Prominent downregulated genes were

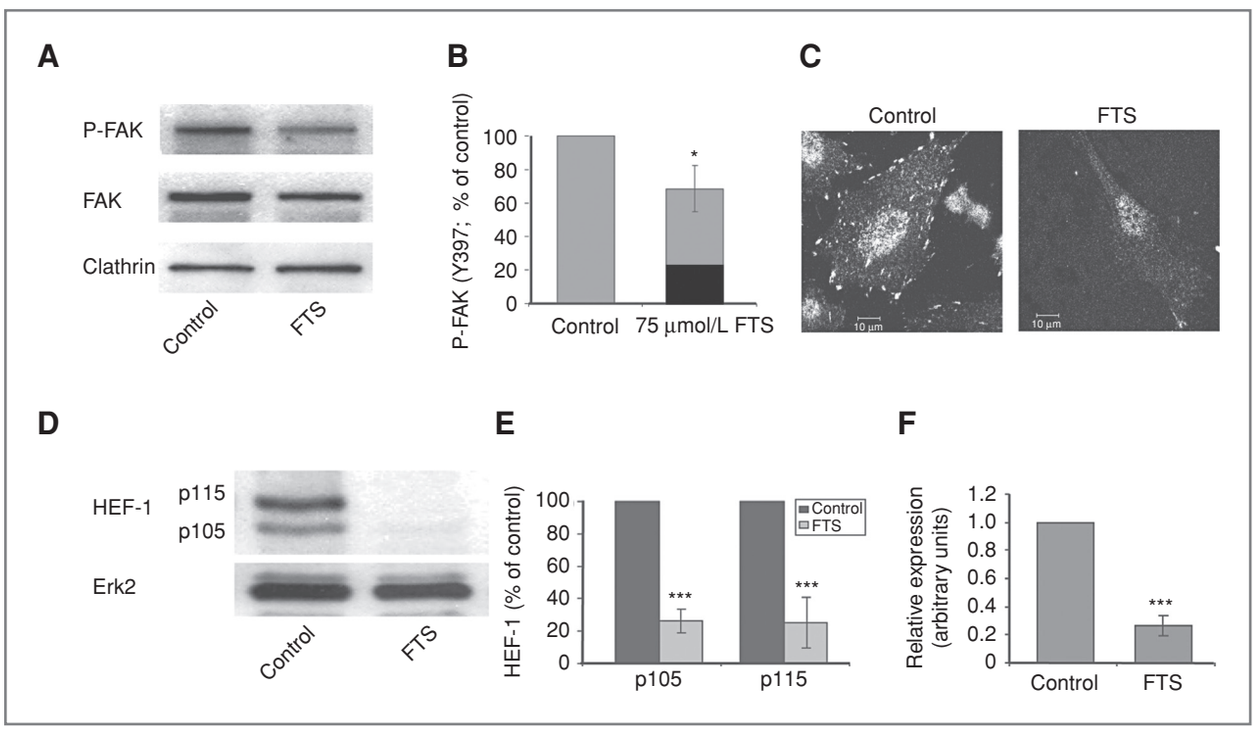

Figure 2. FTS inhibits regulators of spreading and invasiveness. A, typical immunoblots [α-pY397 FAK, α-tFAK, and α-clathrin heavy chain (used here and thereafter as loading control)] of ST88-14 cells treated with FTS (48 hours, 75 μmol/L, 5% FCS) or vehicle. B, quantification of pY397 FAK (% of control; *, $P < 0.05$; $n = 4$). C, typical confocal micrographs (α-pY397 FAK) of the ventral membrane of cells treated as in A. Bars, 10 μm. D, typical immunoblots (α-HEF1 and α-Erk2) of cells treated as in A. P115 is the hyperphosphorylated form of P105. E, quantification of the relative amounts of HEF1 (% of control; ***, $P < 0.001$; $n = 4$). F, qRT-PCR assessment of HEF1 mRNA in FTS-treated or vehicle-treated cells (as in A; ***, $P < 0.001$; $n = 4$).

Published OnlineFirst June 1, 2011; DOI: 10.1158/1535-7163.MCT-10-1087

Table 1. FTS alters the transcriptome of ST88-14 cells and the expression of EMT-related genes

	Term	Count	%	*P*
Upregulated genes	Cell differentiation	705	10.38	E-065.01
	Regulation of cell proliferation	328	4.83	0.02
	Regulation of cell death	323	4.75	0.05
	Cell–cell adhesion	141	2.08	1.05E-05
	Regulation of cell migration	75	1.1	0.01
Downregulated genes	Programmed cell death	261	7.92	0.002
	Establishment of localization in cell	256	7.77	1.34E-04
	Protein transport	216	6.56	5.74E-04
	Regulation of cell proliferation	202	6.13	9.55E-04
	Cell motion	158	4.8	0.004
	Cytoskeleton organization	139	4.22	2.97E-05
	Microtubule cytoskeleton organization	46	1.4	8.43E-04

NOTE: The GO-term analysis of active genes of FTS-treated ST88-14 cells was carried out with the DAVID bioinformatic database using the active genes in the microarray results.

associated with dedifferentiation and cytoskeletal organization such as versican (decreased by 79-fold), β-actin (by 21-fold), ezrin (by 21-fold), HEF1 (by 16-fold), β-tubulin (by 15-fold), and RhoB (by 8.6-fold). Furthermore, expression of TGF-β superfamily members and signal transducers was also decreased: BMP4 (by 30-fold), TGF-β receptor I (by 14-fold), TGF-β1 (by 11.3-fold), and latent TGF-β-binding protein 1 (by 8-fold). In addition, the expression of integrins, protocadherins, protoglycans, MMPs, and cytoskeleton organization proteins was also altered. These results were confirmed by qRT-PCR for a subset of the above-mentioned genes (data not shown).

A DAVID gene ontology analysis (35) revealed that the FTS-mediated upregulation of genes was involved in cell differentiation, cell proliferation, cell death, cell–cell adhesion, and cell migration (Table 1). Complementarily, genes involved in the regulation of metabolic processes, macromolecule biosynthesis, programmed cell death, vesicle-mediated transport, cell cycle and proliferation, angiogenesis, and cytoskeleton organization were downregulated by FTS (Table 1). These results suggested an FTS-induced phenotypic reversion of NF1-deficient ST88-14 cells, analogous to a mesenchymal-to-epithelial transition (MET) of epithelial tumors. Both EMT and MET are closely associated TGF-β-superfamily signaling (3). Here, too, FTS mediated the reduction of TGF-β1 and BMP4 (see above) and of their receptors, TGF-β type I receptor (14-fold) and the BMP type II receptor (3.2-fold). Quantitative qRT-PCR disclosed that FTS induced a dramatic decrease in BMP4 (by 97%, $P < 0.001$, $n = 4$) and a milder reduction in TGF-β1 (to 66% of that in control cells, $P < 0.06$, $n = 3$) transcripts. In these conditions, TGF-β1 protein was also reduced to approximately 60% of that in control cells ($P < 0.01$, $n = 4$). These results suggest the Ras-mediated regulation of TGF-β and BMP4 signaling in NF1-deficient cells.

FTS inhibits BMP4 and TGF-β signaling in NF1-deficient MPNST cells

To directly examine if FTS modulates BMP4 and TGF-β signaling, serum starved ST88-14 cells treated with FTS (5 μmol/L, 24 h) or vehicle were stimulated with TGF-β1 (5 ng/mL, 30 minutes) or BMP4 (50 ng/mL, 60 minutes). In vehicle-treated cells, Smad3 was robustly phosphorylated in response to TGF-β1 stimulation (Fig. 3A and B). This phosphorylation was substantially reduced by FTS (Fig. 3A and B), which also reduced the nuclear translocation of Smad3 (Fig. 3C and D). In vehicle-treated cells, BMP4 induced Smad1/5/8 phosphorylation (Fig. 3E and F) and nuclear translocation (Fig. 3G and H). Both parameters were significantly reduced upon FTS treatment (Fig. 3E–H). The basal activation level of Smad1/5/8 in the presence of serum, but in the absence of exogenous addition of ligand, was also markedly reduced after FTS (48 hours; Fig. 3I and J) or noggin (100–250 ng/mL, 48 hours; not shown) treatments. In these conditions, no differences in the basal Smad3 phosphorylation were detectable (data not shown). As a control for the specificity of FTS, we used reversine (1–5 μmol/L, 48 hours; ref. 36), an inhibitor of monopolar spindle kinase 1, which was devoid of effects on Ras-GTP levels and on the phosphorylation of Smads1/5/8 and 3 (data not shown). To confirm the role of Ras inhibition on TGF-β1 and BMP4 signaling, we overexpressed a dominant-negative mutant of Ras (Ras17N, dnRas) fused to green fluorescent protein (GFP). dnRas induced a mild but significant decrease in the ligand-induced phosphorylation of Smad1/5/8 and in the expression levels of HEF1 (when compared when GFP-transfected cells; Supplementary Fig. S2A and B). In these conditions, pSmad3 was barely detectable without TGFβ-1 stimulation, thus preempting the analysis of the effects of dnRas on its basal activation levels. We conclude that BMP4 signaling is modulated by active Ras and inhibited by FTS.

Published OnlineFirst June 1, 2011; DOI: 10.1158/1535-7163.MCT-10-1087

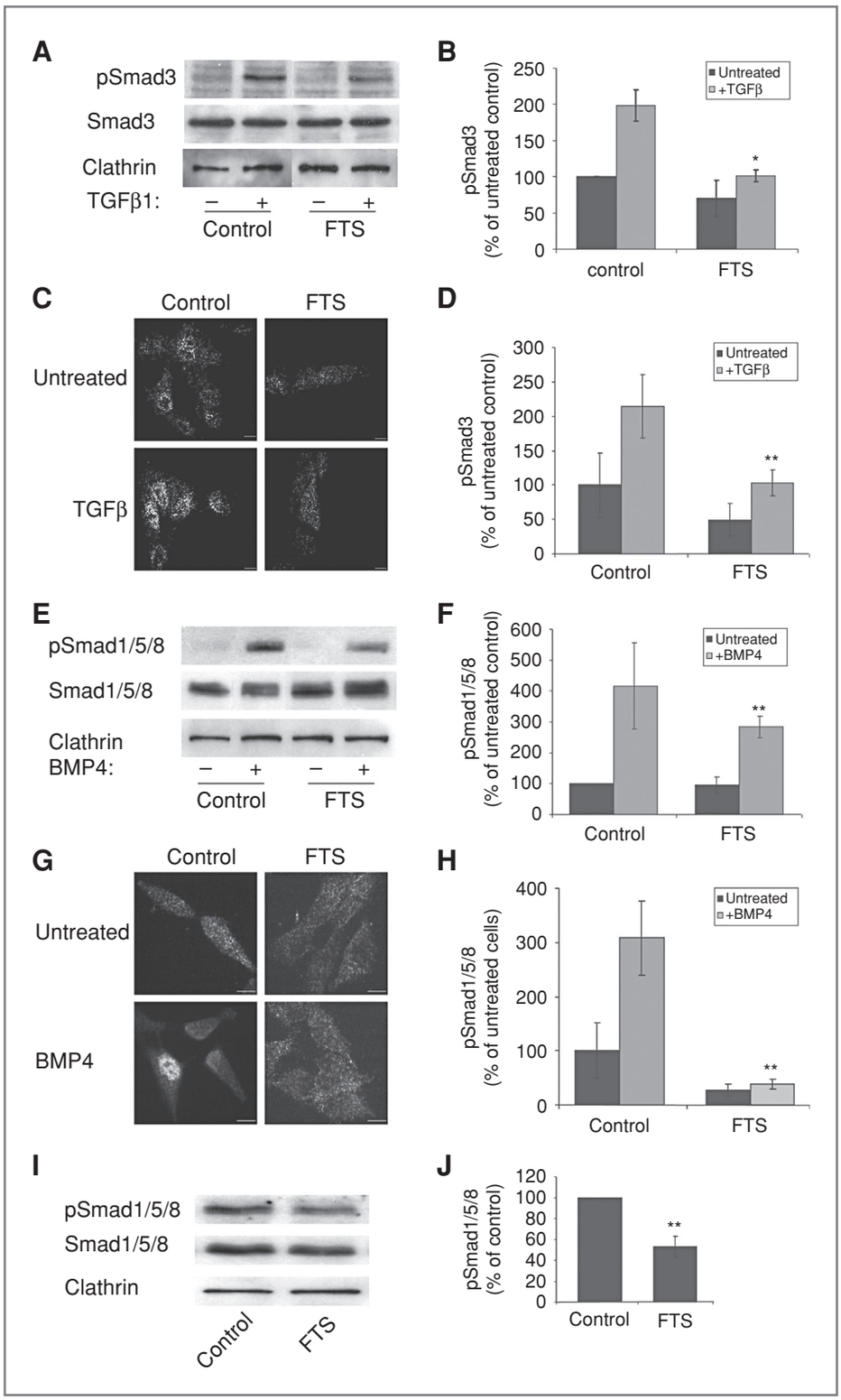

Figure 3. FTS inhibits TGF-β–mediated and BMP4-mediated signaling in ST88-14 cells. A, typical immunoblots (α-pSmad3, α-tSmad3, and α-CHC) of ST88-14 cells treated with FTS (24 hours, 5 μmol/L, 0.1% FCS) or vehicle, unstimulated, or stimulated with TGF-β1 (30 minutes, 5 ng/mL). B, quantification of pSmad3 (% of unstimulated control; *, $P < 0.05$; $n = 3$). C, typical confocal micrographs (α-pSmad3) of cells treated/stimulated as in A. Bars, 10 μm. D, quantification of pSmad3 staining in a typical experiment (% of unstimulated control; **, $P < 0.01$; ~40 cells/condition). E, typical immunoblots (α-pSmad1/5/8, α-tSmad1/5/8, and α-CHC) of ST88-14 cells treated with FTS or vehicle (as in A) and stimulated or not with BMP4 (60 minutes, 50 ng/mL). F, quantification of pSmad1/5/8 (% of unstimulated control; *, $P < 0.01$; $n = 4$). G, typical confocal micrographs (α-pSmad1/5/8) of cells treated/stimulated as in E. Bars, 10 μm. H, quantification of pSmad1/5/8 staining in a typical experiment (% of unstimulated control; **, $P < 0.01$; ~40 cells/condition). I, typical immunoblots (α-pSmad1/5/8, α-tSmad1/5/8, and α-CHC) of ST88-14 cells treated with FTS (48 h, 75 μmol/L, 5% FCS) or vehicle. J, quantification of the relative amounts of pSmad1/5/8 (% of control; **, $P < 0.01$; $n = 4$).

To further investigate the effects of FTS on Smad signaling in MPNSTs, we used the FTS-sensitive NF1-derived T265P21 cells and non-NF1 STS26T cells (20). In both cell lines, FTS significantly reduced the TGF-β–induced phosphorylation of Smad3 (Supplementary Fig. S3A–D). In contrast, the reduction in BMP4-induced

Published OnlineFirst June 1, 2011; DOI: 10.1158/1535-7163.MCT-10-1087

phosphorylation of Smad1/5/8 was significant only in T265P21 cells. Moreover, in T265P21 cells, FTS significantly reduced the basal activation of Smad1/5/8, the expression of HEF1, and the basal activation of Smad3 (Supplementary Fig. S4A and B). These effects were not observed with STS26T cells (Supplementary Fig. S4C and D), suggesting differences between NF1 and non-NF1 MPNSTs. This notion is further supported by results obtained with an additional NF1-derived cell line, 90–8, which were essentially similar to those obtained with T265P21 cells (not shown). FTS also significantly reduced the spreading of T265P21 and STS26T cells (to 75% of control for T265P21, $P < 0.001$; and to 83% of control for STS26T, $P < 0.01$), and reduced wound closure by T265P21 cells in the presence or absence of mitomycin C ($P < 0.001$; Supplementary Fig. S4E and F). The greater effect observed with the NF1-derived cell line is in accord with the notion of the importance of Ras-mediated phenomena in the maintenance of their phenotype.

Direct inhibition of BMP and TGF-β signaling decreases cell spreading

To determine whether BMP4 and/or TGF-β1 activate Ras signaling cascades, we examined the activation of Erk1/2, an established node of cross-talk among these pathways (37) and a regulator of cell spreading and motility (38). BMP4 (50 ng/mL) and TGFβ1 (5 ng/mL) induced a time-dependent activation of Erk, which peaked at 5–10 minutes and decayed by 30 minutes (data not shown), resembling Erk activation by the epidermal growth factor (39). Notably, activation of Erk by BMP4 (5 minutes) was significantly inhibited by FTS (5 μmol/L, 24 hours), suggesting direct cross-talk between Ras and the BMP4-induced pathways (Fig. 4A and B). In contrast,

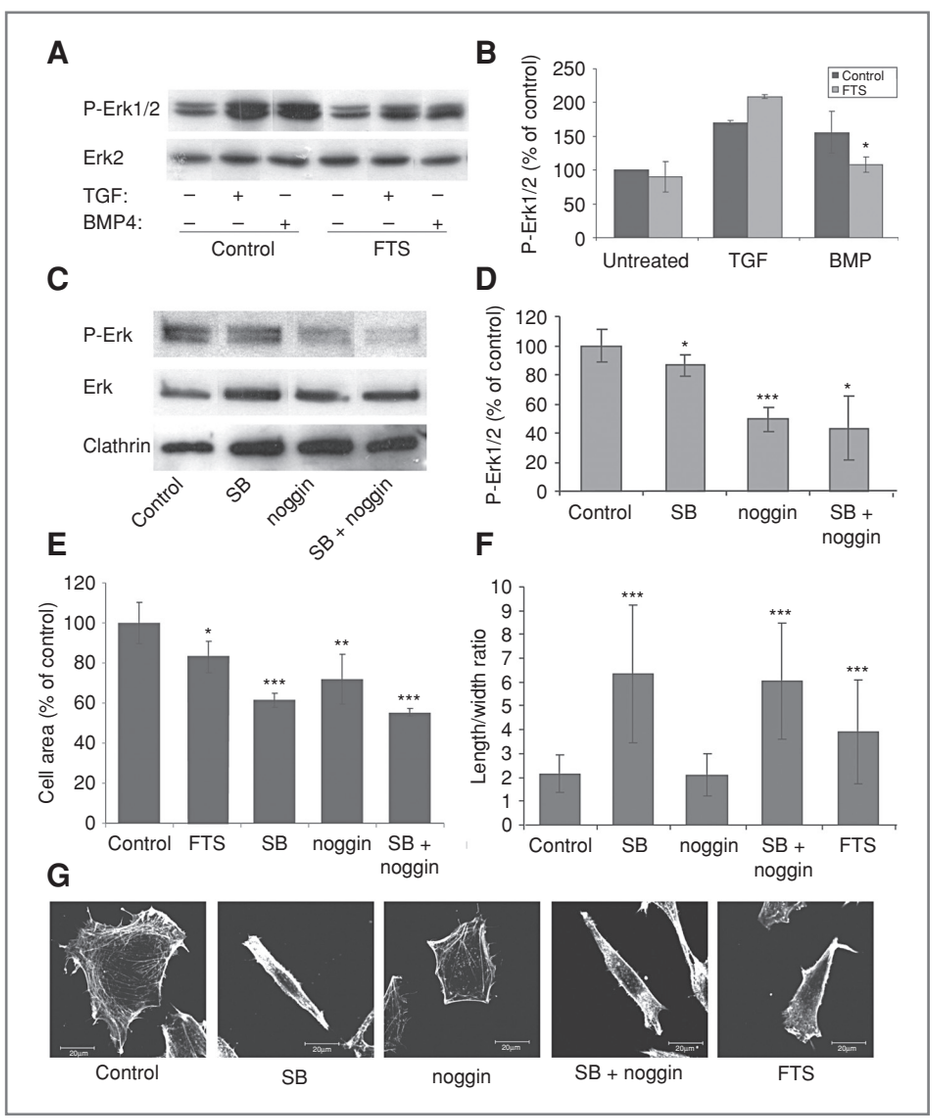

Figure 4. Inhibition of BMP and TGF-β decreases cell spreading. A, representative immunoblots (α-pErk1/2 and α-tErk1/2) of ST88-14 cells treated with FTS (24 hours, 5 μmol/L, 0.1% FCS) or vehicle and stimulated (5 minutes) or not with TGF-β1 (5 ng/mL) or BMP4 (50 ng/mL). B, quantification of the amounts of pErk1/2 (% of unstimulated control; *, $P < 0.05$; $n = 3$). C, representative immunoblots (α-pErk1/2, α-tErk1/2, α-CHC) of serum-starved ST88-14 cells treated (48 hours) with vehicle, SB-431542 (40 μmol/L, SB in figures), noggin (250 ng/mL), or their combination. D, quantification of the amount of pErk1/2 (treatments as in C; *$P < 0.05$; ***$P < 0.001$; $n = 3$). E, ST88-14 cells treated (48 h) with FTS (5 μmol/L), SB-431542 (40 μmol/L), noggin (250 ng/mL), or a combination of SB-431542 and noggin (at the listed concentrations) were assayed for cell spreading (4 hours). Cell areas were calculated with SlideBook. Graph depicts the average cell areas (% of control; *, $P < 0.05$; ***, $P < 0.001$; $n = 3$). F and G, typical confocal micrographs of rhodamine–phalloidin stained ST88-14 cells (treated as in E; bars, 20 μm) and quantification of the length/width ratio of randomly imaged cells (F, $n = 60$ cells/condition; ***, $P < 0.001$).

Published OnlineFirst June 1, 2011; DOI: 10.1158/1535-7163.MCT-10-1087

the induction of Erk phosphorylation by TGF-β1 was not inhibited by FTS (Fig. 4A and B). These results suggest a BMP4/Ras/Erk signaling node and a less direct mode of interaction among TGF-β1–Ras–Erk. We next probed for effects on Erk phosphorylation by the BMP antagonist noggin (250 ng/mL, 48 hours), the TGF-β receptor kinase inhibitor SB-431542 (40 μmol/L, 48 hours), or their combination. SB-431542 weakly inhibited Erk phosphorylation. In contrast, noggin reduced pErk by 50% (Fig. 4C and D), an inhibition that was not enhanced by inhibitor combination (Fig. 4C and D). These results suggest the prominence of BMP4-mediated phenomena, in ST88-14 cells, in constitutive Erk activation, whereas TGF-β may exert different functions.

To examine the roles of BMPs and TGF-β in the spreading of ST88-14 cells, we inhibited both pathways (as above) and found that the inhibition of their signaling significantly decreased cell spreading [by ∼39% (SB-431542), ∼28% (noggin), and ∼45% (SB421542 + noggin), $P < 0.001$, $n = 3$; Fig. 4E]. These cell spreading assays address the initial spreading of adhered cells and do not address steady-state cell morphology or quantitate cell adhesion. Next, we examined the effects of inhibition of BMP, TGF-β, or Ras on cell morphology. The tendency toward spindle morphology was quantified by correlating the length and widths of serum-starved ST88-14 cells upon different treatments (48 hours, 40 μmol/L SB-431542, 250 ng/mL noggin, 5 μmol/L FTS; Fig. 4F and G). In these conditions, SB-431542 and FTS augmented the tendency toward a spindle-like appearance (Fig. 4F and G). In contrast, noggin had no effect on the acquisition of a spindle-like shape, suggesting that Ras and TGF-β, but not BMPs, regulate processes related to the steady state morphology of ST88-14 cells.

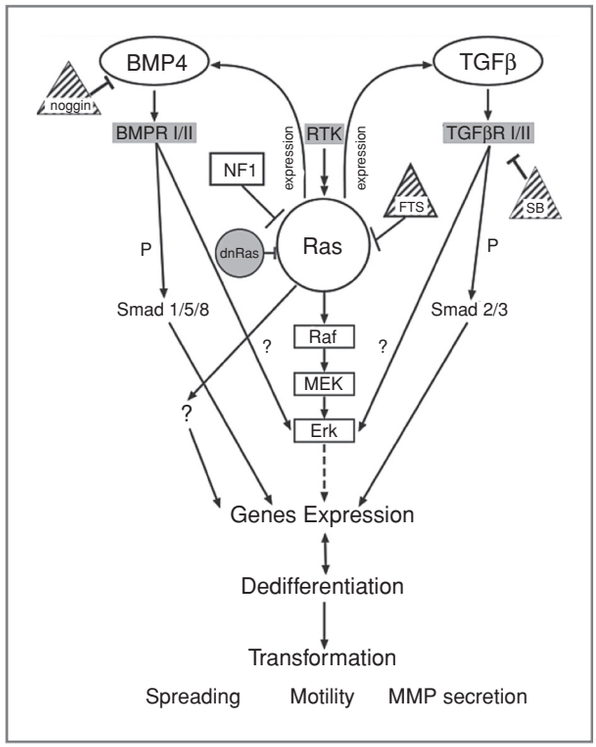

Figure 5. Proposed model. NF1-deficient MPNSTs are endowed with constitutively activated Ras. Active Ras drives the Raf/MEK/Erk signaling, and the activation of the BMP4 and TGF-β signaling pathways, at least partially through alterations in gene expression, including the upregulation of BMP4 and TGF-β. The concomitant activation of BMP4 and TGF-β pathways activates Smad-mediated signaling and Erk, substantiates the alterations in gene expression, and promotes dedifferentiation of NF1-deficient MPNSTs. Blockage of Ras signaling by FTS reverses this sequence of events and leads to redifferentiation and a reduction in tumorigenicity. Direct blockage of BMP4 and TGF-β signaling by noggin and SB431542, respectively, alters Erk activation as well as different aspects of the interaction of MPNSTs with the matrix.

Discussion

Here, we show that phenotypic attributes of NF1-deficient cells involve the deregulation of Ras signaling in conjuncture with signaling mediated by BMP4 and TGF-β. A model depicting the integration of these signaling pathways and the inhibitory effect exerted by FTS or dnRas (on Ras activation), noggin, and SB-431542 is shown in Fig. 5.

FTS inhibited motility and gelatinase secretion of ST88-14 cells (Fig. 1) and the spreading of 3 MPNST cell lines (Fig. 1; data not shown). High levels of spreading, motility, and gelatinase secretion are hallmarks of invasive tumors and are associated with Ras activation (38). FTS also inhibited Rac activation, FAK phosphorylation and localization, and the expression and phosphorylation of HEF1 (Fig. 2; Supplementary Fig. S3), all of which correlate with tumor invasiveness and metastasis (29, 33). Gene expression analysis disclosed that the FTS-induced alterations occurred in the context of an extensive phenotypic alteration involving the transcriptional activation/repression of 3,166 genes (Table 1). This alteration included target genes of the TGF-β superfamily, suggestive of a regulatory role for TGF-β and BMP signaling in determining the phenotype of NF1-deficient MPNSTs. Accordingly, FTS inhibited Smad1/5/8 and Smad3 phosphorylation and nuclear translocation induced by BMP4 and TGF-β1, respectively (Fig. 3A–F; Supplementary Fig. S3). Notably, the constitutive phosphorylation of Smad1/5/8, observed in 5% FCS, was also diminished by FTS (Fig. 3I and J) and dnRas (Supplementary Fig. S3). FTS also reduced the BMP4-induced phosphorylation of Erk (Fig. 4A and B). Accordingly, direct inhibition of BMP4 with noggin reduced Erk phosphorylation and cell spreading (Fig. 4C–E), both of which are sensitive to FTS and thus Ras dependent (Figs. 1 and 4). Also, FTS and the TGF-β receptor kinase inhibitor SB-431542 reduced cell spreading and induced analogous alterations to cell morphology (Fig. 4E–G). Taken together, the here-presented results and our earlier data (20) indicate that Ras inhibition through FTS inhibits MPNST proliferation and transformation, and alters their phenotype through modifications to BMP4 and TGF-β signaling.

Published OnlineFirst June 1, 2011; DOI: 10.1158/1535-7163.MCT-10-1087

The extent and robustness of the FTS-mediated phenotypic alterations to MPNSTs are reminiscent of an MET of epithelial tumors. In cancer-related EMT, overactivation of tumor-related signaling pathways overrides the differentiation program of the cell of origin. Our results support a similar scenario in MPNSTs. A BMP4-induced EMT occurs in the delamination and migration of neural crest cells in development (5). The role of BMP4 in this developmental process and the here-observed constitutive activation of this pathway in NF1-deficient cells (Fig. 3I and J; Supplementary Fig. S3A and B) suggest that similar mechanisms may operate in phenotypic transitions in malignant and developmental settings. Importantly, the induction and maintenance of the mesenchymal/invasive phenotype may involve Ras signaling. Indeed, in NF1-deficient cells, Ras effectors were implicated in the expression of EMT-related genes and the induction of an invasive phenotype (40).

Our results strengthen the previously observed convergence of Ras and TGF-β/BMP signaling pathways (41). Thus, all 3 pathways converge in the activation of mitogen-activated protein kinases (MAPK) and stress-activated protein kinases (42). Here, we observed Erk activation in response to BMP4 and TGF-β1 in MPNSTs. Ras may promote or abrogate different aspects of TGF-β/BMP signaling (10, 11, 43). Importantly, in mouse mammary epithelial cells, the Ras/Raf/MEK/Erk signaling is necessary for the TGF-β–mediated induction of EMT tumorigenesis enhancement (44). We suggest an aggressiveness-promoting cross-talk among these pathways in the context of NF1-deficient MPNSTs.

In Schwann cells, activation of Ras/Raf/MEK/Erk drives dedifferentiation, pivotal in the development of $NF1^{-/-}$ neurofibromas (21). Similarly, MAPKs are crucial signaling nodes and regulate the acquisition of multiple tumorigenic attributes (45). The here-observed activation of Erk by BMP4 (Fig. 4A and B), inhibition of this activation by both noggin and FTS (Fig. 4A–D), and the inhibitory effects of these treatments on cell spreading (Fig. 4E) reinforce the notion of Erk as an integrator of morphogenic and mitogenic signaling pathways in $NF1^{-/-}$ cells (see schematic depiction; Fig. 5).

Of note, similar to the diversity of BMP4-induced effects in development, which range from the induction of neural crest differentiation and delamination (6) to the induction of terminal differentiation and apoptosis (46), BMP4 may also exert diverse effects in the context of tumors. Thus, in contrast to the here-reported promotion of the transformation of NF1-deficient cells, a tumor-inhibitory role was proposed for BMP4 in the context of tumor-initiating precursors of glioblastoma (47). Future studies will be centered on clarifying the effects of the BMP and TGF-β pathways on the tumorigenic potential of MPNSTs *in vivo* and on the potential therapeutic benefits of the combinations of inhibitors of the 3 pathways.

Disclosure of Potential Conflicts of Interest

No potential conflicts of interest were disclosed.

Acknowledgments

We thank S.R. Smith for editorial assistance; Dr. Jasmine Jacob-Hirsch, and Prof. Gideon Rechavi (The Chaim Sheba Medical Center, Tel Hashomer, Israel) for expert advice on the DNA-chip analysis.

Grant Support

We acknowledge support from the Israel Science Foundation (912/06, Y. Kloog and 1122/06, M. Ehrlich) and the Prajs-Drimmer Institute for The Development of Antidegenerative Drugs.

The costs of publication of this article were defrayed in part by the payment of page charges. This article must therefore be hereby marked *advertisement* in accordance with 18 U.S.C. Section 1734 solely to indicate this fact.

Received December 5, 2010; revised April 28, 2011; accepted May 20, 2011; published OnlineFirst June 1, 2011.

References

1. Vicente-Duenas C, Gutierrez de Diego J, Rodriguez FD, Jimenez R, Cobaleda C. The role of cellular plasticity in cancer development. Curr Med Chem 2009;16:3676–85.
2. DeNicola GM, Tuveson DA. RAS in cellular transformation and senescence. Eur J Cancer 2009;45 Suppl 1:211–6.
3. Miyazono K. Transforming growth factor-beta signaling in epithelial-mesenchymal transition and progression of cancer. Proc Jpn Acad Ser B Phys Biol Sci 2009;85:314–23.
4. Bailey JM, Singh PK, Hollingsworth MA. Cancer metastasis facilitated by developmental pathways: Sonic hedgehog, Notch, and bone morphogenic proteins. J Cell Biochem 2007;102:829–39.
5. Thiery JP, Sleeman JP. Complex networks orchestrate epithelial-mesenchymal transitions. Nat Rev Mol Cell Biol 2006;7:131–42.
6. Sela-Donenfeld D, Kalcheim C. Regulation of the onset of neural crest migration by coordinated activity of BMP4 and Noggin in the dorsal neural tube. Development 1999;126:4749–62.
7. Deng H, Makizumi R, Ravikumar TS, Dong H, Yang W, Yang WL. Bone morphogenetic protein-4 is overexpressed in colonic adenocarcinomas and promotes migration and invasion of HCT116 cells. Exp Cell Res 2007;313:1033–44.
8. Theriault BL, Shepherd TG, Mujoomdar ML, Nachtigal MW. BMP4 induces EMT and Rho GTPase activation in human ovarian cancer cells. Carcinogenesis 2007;28:1153–62.
9. Gotzmann J, Mikula M, Eger A, Schulte-Hermann R, Foisner R, Beug H, et al. Molecular aspects of epithelial cell plasticity: implications for local tumor invasion and metastasis. Mutat Res 2004;566:9–20.
10. Mulder KM. Role of Ras and Mapks in TGFbeta signaling. Cytokine Growth Factor Rev 2000;11:23–35.
11. Kfir S, Ehrlich M, Goldshmid A, Liu X, Kloog Y, Henis YI. Pathway- and expression level-dependent effects of oncogenic N-Ras: p27(Kip1) mislocalization by the Ral-GEF pathway and Erk-mediated interference with Smad signaling. Mol Cell Biol 2005;25:8239–50.
12. Bos JL. ras oncogenes in human cancer: a review. Cancer Res 1989;49:4682–9.
13. Stephens K, Riccardi VM, Rising M, Ng S, Green P, Collins FS, et al. Linkage studies with chromosome 17 DNA markers in 45 neurofibromatosis 1 families. Genomics 1987;1:353–7.
14. Hirota S, Nomura S, Asada H, Ito A, Morii E, Kitamura Y. Possible involvement of c-kit receptor and its ligand in increase of mast cells in neurofibroma tissues. Arch Pathol Lab Med 1993;117:996–9.

Published OnlineFirst June 1, 2011; DOI: 10.1158/1535-7163.MCT-10-1087

15. Ferner RE, Gutmann DH. International consensus statement on malignant peripheral nerve sheath tumors in neurofibromatosis. Cancer Res 2002;62:1573–7.
16. Hiatt KK, Ingram DA, Zhang Y, Bollag G, Clapp DW. Neurofibromin GTPase-activating protein-related domains restore normal growth in Nf1-/- cells. J Biol Chem 2001;276:7240–5.
17. Cawthon RM, Weiss R, Xu GF, Viskochil D, Culver M, Stevens J, et al. A major segment of the neurofibromatosis type 1 gene: cDNA sequence, genomic structure, and point mutations. Cell 1990;62: 193–201.
18. Ballester R, Marchuk D, Boguski M, Saulino A, Letcher R, Wigler M, et al. The NF1 locus encodes a protein functionally related to mammalian GAP and yeast IRA proteins. Cell 1990;63:851–9.
19. Kloog Y, Cox AD. RAS inhibitors: potential for cancer therapeutics. Mol Med Today 2000;6:398–402.
20. Barkan B, Starinsky S, Friedman E, Stein R, Kloog Y. The Ras inhibitor farnesylthiosalicylic acid as a potential therapy for neurofibromatosis type 1. Clin Cancer Res 2006;12:5533–42.
21. Harrisingh MC, Perez-Nadales E, Parkinson DB, Malcolm DS, Mudge AW, Lloyd AC. The Ras/Raf/ERK signalling pathway drives Schwann cell dedifferentiation. EMBO J 2004;23:3061–71.
22. Yang FC, Chen S, Clegg T, Li X, Morgan T, Estwick SA, et al. Nf1+/- mast cells induce neurofibroma like phenotypes through secreted TGF-beta signaling. Hum Mol Genet 2006;15:2421–37.
23. Benard V, Bohl BP, Bokoch GM. Characterization of rac and cdc42 activation in chemoattractant-stimulated human neutrophils using a novel assay for active GTPases. J Biol Chem 1999;274:13198–204.
24. Haklai R, Gana-Weisz G, Elad G, Paz A, Marciano D, Egozi Y, et al. Dislodgment and accelerated degradation of Ras. Biochemistry 1998;37:1306–14.
25. Rotblat B, Ehrlich M, Haklai R, Kloog Y. The Ras inhibitor farnesylthiosalicylic acid (Salirasib) disrupts the spatiotemporal localization of active Ras: a potential treatment for cancer. Methods Enzymol 2008;439:467–89.
26. Shapira S, Barkan B, Fridman E, Kloog Y, Stein R. The tumor suppressor neurofibromin confers sensitivity to apoptosis by Ras-dependent and Ras-independent pathways. Cell Death Differ 2006.
27. Lambert JM, Lambert QT, Reuther GW, Malliri A, Siderovski DP, Sondek J, et al. Tiam1 mediates Ras activation of Rac by a PI(3)K-independent mechanism. Nat Cell Biol 2002;4:621–5.
28. Ingram DA, Hiatt K, King AJ, Fisher L, Shivakumar R, Derstine C, et al. Hyperactivation of p21(ras) and the hematopoietic-specific Rho GTPase, Rac2, cooperate to alter the proliferation of neurofibromin-deficient mast cells in vivo and in vitro. J Exp Med 2001; 194:57–69.
29. Tomar A, Schlaepfer DD. Focal adhesion kinase: switching between GAPs and GEFs in the regulation of cell motility. Curr Opin Cell Biol 2009;21:676–83.
30. Boyanapalli M, Lahoud OB, Messiaen L, Kim B, Anderle de Sylor MS, Duckett SJ, et al. Neurofibromin binds to caveolin-1 and regulates ras, FAK, and Akt. Biochem Biophys Res Commun 2006;340:1200–8.
31. Grove M, Komiyama NH, Nave KA, Grant SG, Sherman DL, Brophy PJ. FAK is required for axonal sorting by Schwann cells. J Cell Biol 2007;176:277–82.
32. Law SF, Estojak J, Wang B, Mysliwiec T, Kruh G, Golemis EA. Human enhancer of filamentation 1, a novel p130cas-like docking protein, associates with focal adhesion kinase and induces pseudohyphal growth in Saccharomyces cerevisiae. Mol Cell Biol 1996;16:3327–37.
33. O'Neill GM, Seo S, Serebriiskii IG, Lessin SR, Golemis EA. A new central scaffold for metastasis: parsing HEF1/Cas-L/NEDD9. Cancer Research 2007;67:8975–9.
34. ArrayExpress. Available from: http://www.ebi.ac.uk/microarray-as/ae/.
35. DAVID functional annotation bioinformatics microarray analysis [internet]: DAVID bioinformatics resources 6.7, National Institute of Allergy and Infectious Diseases (NIAID), NIH. Available from: http://david.abcc.ncifcrf.gov/.
36. Chen S, Zhang Q, Wu X, Schultz PG, Ding S. Dedifferentiation of lineage-committed cells by a small molecule. J Am Chem Soc 2004;126:410–1.
37. Giehl K, Imamichi Y, Menke A. Smad4-independent TGF-beta signaling in tumor cell migration. Cells Tissues Organs 2007;185:123–30.
38. Liotta LA. Gene products which play a role in cancer invasion and metastasis. Breast Cancer Res Treat 1988;11:113–24.
39. Marshall CJ. Specificity of receptor tyrosine kinase signaling: transient versus sustained extracellular signal-regulated kinase activation. Cell 1995;80:179–85.
40. Bodempudi V, Yamoutpoor F, Pan W, Dudek AZ, Esfandyari T, Piedra M, et al. Ral overactivation in malignant peripheral nerve sheath tumors. Mol Cell Biol 2009;29:3964–74.
41. Javelaud D, Mauviel A. Crosstalk mechanisms between the mitogen-activated protein kinase pathways and Smad signaling downstream of TGF-beta: implications for carcinogenesis. Oncogene 2005;24: 5742–50.
42. Miyazono K, Maeda S, Imamura T. BMP receptor signaling: transcriptional targets, regulation of signals, and signaling cross-talk. Cytokine Growth Factor Rev 2005;16:251–63.
43. Beck SE, Carethers JM. BMP suppresses PTEN expression via RAS/ERK signaling. Cancer Biol Ther 2007;6:1313–7.
44. Janda E, Lehmann K, Killisch I, Jechlinger M, Herzig M, Downward J, et al. Ras and TGF[beta] cooperatively regulate epithelial cell plasticity and metastasis: dissection of Ras signaling pathways. J Cell Biol 2002;156:299–313.
45. Whyte J, Bergin O, Bianchi A, McNally S, Martin F. Key signalling nodes in mammary gland development and cancer. Mitogen-activated protein kinase signalling in experimental models of breast cancer progression and in mammary gland development. Breast Cancer Res 2009;11:209.
46. Mehler MF, Mabie PC, Zhang D, Kessler JA. Bone morphogenetic proteins in the nervous system. Trends Neurosci 1997;20:309–17.
47. Piccirillo SG, Reynolds BA, Zanetti N, Lamorte G, Binda E, Broggi G, et al. Bone morphogenetic proteins inhibit the tumorigenic potential of human brain tumour-initiating cells. Nature 2006;444:761–5.